8078 *Inorg. Chem.* **2009**, *48*, 8078–8080
DOI: 10.1021/ic9013653

Inorganic Chemistry
Communication

Stability of a Ferryl−Peptide Conjugate Is Controlled by a Remote Substituent

Nitinkumar D. Jabre, Lew Hryhorczuk, and Jeremy J. Kodanko*

Department of Chemistry and Central Instrumentation Facility, Wayne State University, 5101 Cass Avenue, Detroit, Michigan 48202

Received July 13, 2009

The formation of a synthetic ferryl−peptide conjugate and mechanistic studies that elucidate its mode of decomposition are presented. A ferryl species is generated from a ligand−dipeptide conjugate **4**. The ferryl species $[Fe^{IV}(\mathbf{4})(O)]^{2+}$, noted as compound **5**, was characterized by UV−vis spectroscopy and by high-resolution electrospray mass spectrometry. The ferryl−peptide conjugate **5** is stable for over 1 h at room temperature. Ester derivatives of **5** decay at different rates, consistent with the remote ester group controlling the stability of the ferryl. The kinetic isotope effect value (4.5) and $\rho = -1.3$ observed with ester derivatives suggest that the mechanism for decomposition of **5** follows a hydrogen-atom-transfer pathway. The formation and decay of **5** was fit to a two-step process, with the decay being unimolecular with respect to the ferryl **5**.

High-valent iron(IV) oxo species, also known as ferryls, are found in enzymes that carry out oxidation reactions in nature.[1,2] Ligands that mimic the active sites of these enzymes can be used to generate biomimetic ferryl species[3,4] that oxidize a variety of organic molecules in an intermolecular fashion.[5,6] In contrast, reactions of ferryls tethered to organic substrates have received little attention.[7,8] In fact, it is not currently understood which functional groups are compatible with a ferryl in a complex molecule. This is unfortunate because these data are relevant to the understanding of which functionalities would be tolerated in synthetic catalysts or artifical oxygenases that generate ferryl species. In this Communication, we report the interesting observation that the stability of a ferryl−peptide conjugate can be controlled by a remote functional group that is 11 atoms removed from the iron center. In addition, reported mechanistic studies support an intramolecular decay pathway for the ferryl−peptide conjugate.

In order to synthesize the ferryl−peptide conjugate, synthetic methodology was developed for attaching pentadentate ligands like N4Py to an alanine side chain. Toward this goal, the unnatural amino acid **2**, hydroxymethylpyridylalanine (HPA), was synthesized in racemic form in two steps starting from bromide **1** using phase-transfer alkylation as the key step (Scheme 1).[9] After acetylation, the unnatural amino acid was incorporated into dipeptide **3** upon coupling with H-Gly-OBn. Attaching the remainder of the metal-binding group was accomplished by transforming the silyloxy group of **3** into a chloride, followed by displacement with the secondary amine $NH(CH_2Py)(CHPy_2)$ (where Py = 2-pyridyl). Installation of the metal-binding unit in the last step was ideal because it maximized the divergence of the synthesis. Furthermore, this approach holds the advantage that the amino acid **2** can be placed at varied positions along a peptide chain.

To form the ferrous complex of the peptide, a solution of **4** in H_2O/CH_3CN (1:1) was treated with 1 equiv of $Fe^{II}(ClO_4)_2$ to generate the species in situ. Spectral data for $[Fe^{II}(\mathbf{4})(CH_3CN)]^{2+}$ are in good agreement with those for the parent ligand N4Py in the same solvent mixture (Table S1 in the Supporting Information, SI). The complex $[Fe^{II}(\mathbf{4})(CH_3CN)]^{2+}$ was characterized by UV−vis ($\varepsilon_{380} = 4200\ M^{-1}\ cm^{-1}$ and $\varepsilon_{455} = 3600\ M^{-1}\ cm^{-1}$) and NMR spectroscopy, as well as by electrospray mass spectrometry (ESMS; Figures S1 and S2 in the SI). All resonances in the NMR spectrum of $[Fe^{II}(\mathbf{4})(CH_3CN)]^{2+}$ lie between 10 and 0 ppm, consistent with the ferrous complex being in the low-spin state.

The ferrous complex $[Fe^{II}(\mathbf{4})(CH_3CN)]^{2+}$ was used to generate a ferryl with impressive stability, considering the weak C−H bonds present in the peptide placed in close proximity to the iron center. Treatment of $[Fe^{II}(\mathbf{4})(CH_3CN)]^{2+}$ with $KHSO_5$ at 25 °C generated a pale-green species, noted as compound **5**, with a maximum absorption wavelength at

*To whom correspondence should be addressed. E-mail: jkodanko@chem.wayne.edu.

(1) Krebs, C.; Fujimori, D. G.; Walsh, C. T.; Bollinger, J. M. Jr. *Acc. Chem. Res.* **2007**, *40*, 484–492.
(2) Costas, M.; Mehn, M. P.; Jensen, M. P.; Que, L. Jr. *Chem. Rev.* **2004**, *104*, 939–986.
(3) Que, L. *Acc. Chem. Res.* **2007**, *40*, 493–500.
(4) Nam, W. *Acc. Chem. Res.* **2007**, *40*, 522–531.
(5) Kaizer, J.; Klinker, E. J.; Oh, N. Y.; Rohde, J.-U.; Song, W. J.; Stubna, A.; Kim, J.; Münck, E.; Nam, W.; Que, L. Jr. *J. Am. Chem. Soc.* **2004**, *126*, 472–473.
(6) van den Berg, T. A.; de Boer, J. W.; Browne, W. R.; Roelfes, G.; Feringa, B. L. *Chem. Commun.* **2004**, 2550–2551.
(7) Jensen, M. P.; Lange, S. J.; Mehn, M. P.; Que, E. L.; Que, L. Jr. *J. Am. Chem. Soc.* **2003**, *125*, 2113–2128.
(8) For characterization of an $Fe^{III}(OOH)$ species derived from N4Py bound to a peptide, see: (a) Choma, C. T.; Schudde, E. P.; Kellogg, R. M.; Robillard, G. T.; Feringa, B. L. *J. Chem. Soc., Perkin Trans. 1* **1998**, 769–774. (b) van den Heuvel, M.; van den Berg, T. A.; Kellogg, R. M.; Choma, C. T.; Feringa, B. L. *J. Org. Chem.* **2004**, *69*, 250–262.
(9) The enantioselective synthesis of **2** will be reported elsewhere.

 Published on Web 07/31/2009

Scheme 1. Synthesis of Ligand−Peptide Conjugate **4**[a]

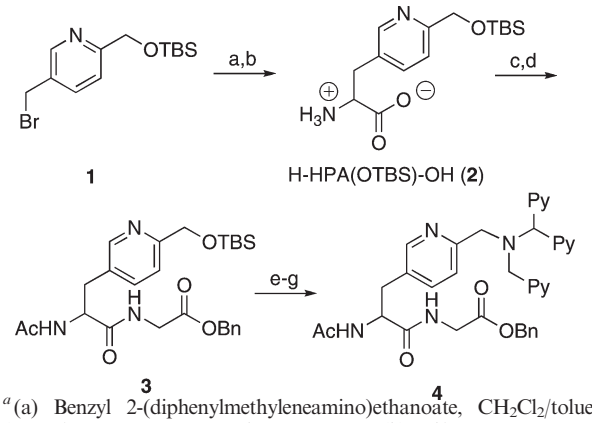

[a] (a) Benzyl 2-(diphenylmethyleneamino)ethanoate, CH_2Cl_2/toluene (3:7), TBAH, 50% NaOH, 4 h, 0 °C, 88%; (b) Pd/C, MeOH, rt, 6 h, 77%; (c) Ac_2O, Et_3N, CH_2Cl_2, rt, 4 h, quantitative; (d) H-Gly-OBn, EDAC, HOBt, Et_3N, CH_2Cl_2, rt, 18 h, 72%; (e) TBAF, AcOH, THF, rt, 1.5 h, 76%; (f) LiCl, *i*Pr_2EtN, TsCl, CH_3CN, 0 °C to rt, 6 h, 70%; (g) NH(CH_2Py)-($CHPy_2$), *i*Pr_2EtN, NaI (catalyst), CH_3CN, 55 °C, 24 h, 90%.

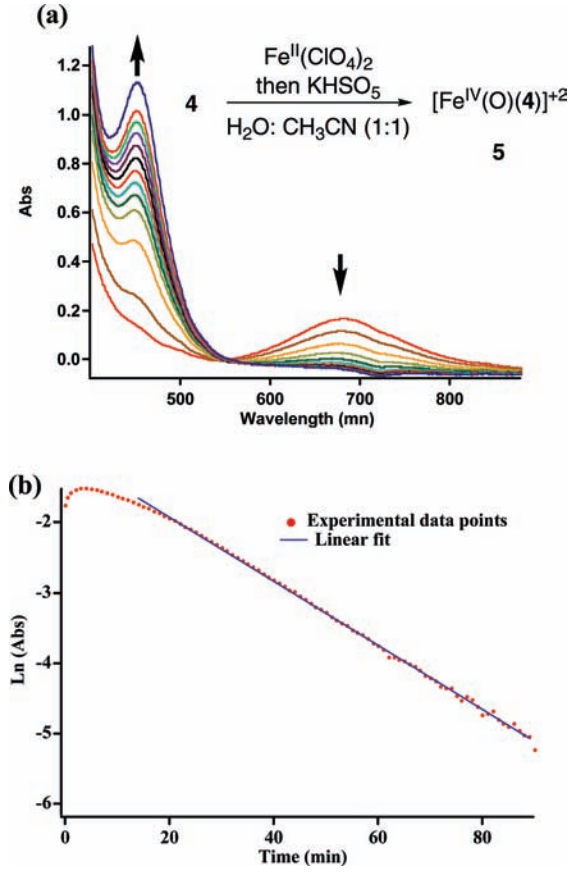

Figure 1. (a) Decomposition of the ferryl−peptide conjugate $[Fe^{IV}(O)(\mathbf{4})]^{2+}$ (**5**) monitored by UV−vis spectroscopy. The decrease in λ_{max} = 680 nm and increase in λ_{max} = 450 nm corresponds to the decomposition of Fe^{IV} and regeneration of Fe^{II}, respectively. (b) Plot of ln(Abs) at 680 nm vs time (red) and linear fit (blue) for species **5** ([Fe] = 1.67 mM).

λ_{max} = 680 nm (Figure 1a), identical with that obtained for the species $[Fe^{IV}(O)(N4Py)]^{2+}$.[10,11] This absorption at 680 nm maximizes after approximately 10 min and then decays via a first-order process, as evidenced by the linearity of the ln(Abs) vs time plot (Figure 1b). The induction period (~10 min) indicates that formation of **5** occurs along with decay at early time points. Therefore, **5** is never fully generated. Extrapolation of the linear portion of the plot in Figure 1b to $t = 0$ allows the calculation of an extinction coefficient for **5** (ε_{680} = 200 M^{-1} cm^{-1}), which is consistent with data for $[Fe^{IV}(O)(N4Py)]^{2+}$ under the same conditions (Table S1 in the SI). The high-resolution ESMS spectrum for **5** has a dominant molecular ion at m/z 357.6093, along with a suitable isotopic pattern, which matches the formula $[Fe^{IV}(O)(\mathbf{4})]^{2+}$ (**5**; Figure S2 in the SI). This molecular ion appears and then disappears on the same time scale as the absorption at 680 nm, consistent with its assignment as the ferryl species.

Although an isosbestic point at 550 nm was observed, the Fe^{II} species (λ_{max} at 450 nm) was not fully regenerated after the decay process, indicating that partial destruction of the metal-binding unit occurred. MS and NMR analysis of the decomposition products revealed that a complex mixture was formed. Several products were identified, including dipyridyl ketone (25%), from oxidative decomposition of the N4Py metal-binding unit,[12] the free acid derived from **4** (32%) and benzaldehyde (8%), consistent with oxidation of the ester substituent (Scheme S1 in the SI). The reactivity of **5** encouraged us to investigate the mechanism of decomposition further in order to pinpoint the group responsible for quenching the ferryl species on the peptide.

Derivatives of the ferryl−peptide conjugate **5** were synthesized in order to determine if a functional group(s) contained in **5** controlled the rate of decomposition (Table 1). The ferryl generated from methyl ester derivative **6** was found to be 12 times more stable than **5**, clearly implicating the role of the benzyl moiety in controlling the decomposition. To test this hypothesis further, the benzyl group was replaced by benzyl-d_7 (**7**). The species $[Fe^{IV}(O)(\mathbf{7})]^{2+}$ decomposed much slower than **5**, giving a kinetic isotope effect (KIE) of 4.5,

Table 1. Observed and Relative Rate Constants for the Decomposition of Ferryl−Peptide Conjugates Generated from Various Ester Derivatives

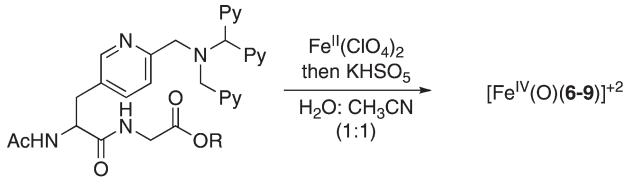

entry	R	rate (s^{-1})[a]	k_{rel}
1	−Bn (**4**)	7.3(6) × 10^{-4}	1.0
2	−Me (**6**)	6.3(3) × 10^{-5}	0.086
3	$-CD_2C_6D_5$ (**7**)	1.6(2) × 10^{-4}	0.22
4	$-CH_2C_6H_4$-*p*-OMe (**8**)	1.6(3) × 10^{-3}	2.2
5	$-CH_2C_6H_4$-*p*-Me (**9**)	1.2(2) × 10^{-3}	1.6
6	$-CH_2C_6H_4$-*p*-Cl (**10**)	3.6(2) × 10^{-4}	0.49

[a] Rates were determined from the slope of ln(Abs) vs time plots. The number reported is the average of at least three runs; the error as the standard deviation is given in parentheses.

(10) Sastri, C. V.; Seo, M. S.; Park, M. J.; Kim, K. M.; Nam, W. *Chem. Commun.* **2005**, 1405–1407.
(11) Klinker, E. J.; Kaizer, J.; Brennessel, W. W.; Woodrum, N. L.; Cramer, C. J.; Que, L. Jr. *Angew. Chem., Int. Ed.* **2005**, *44*, 3690–3694.
(12) Abouelatta, A. I.; Campanali, A. A.; Ekkati, A. R.; Shamoun, M.; Kalapugama, S.; Kodanko, J. J. *Inorg. Chem.* **2009**, ASAP.

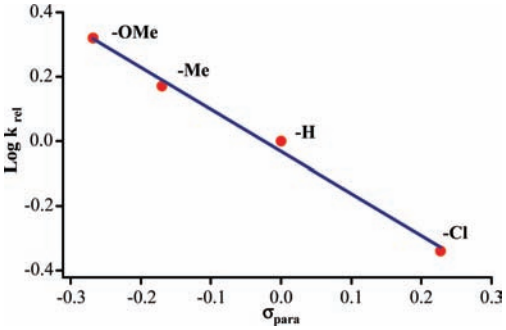

Figure 2. Hammett plot derived from decomposition rates of benzyl ester derivatives **4** and **8**−**10** ($\rho = -1.3$; $r = 0.99$).

strikingly similar to the KIE of 4.4 observed for oxidative dealkylation of ethyl esters by the heme protein cytochrome P-450.[13] Three additional para-X-substituted benzyl ester derivatives (**8**−**10**) were tested, and their rates of decomposition were used to construct a Hammett plot (Figure 2). A strong linear correlation ($r = 0.99$) between σ_p and $\log k_{rel}$ was obtained, giving a ρ value of −1.3. The small ρ value suggests abstraction of a benzylic hydrogen atom by the ferryl group of **5** rather than reaction of the ferryl with the aromatic ring, where a more negative ρ value would be expected.[14] The ρ value is similar to that observed in the oxidation of para-substituted toluene derivatives by cytochrome P-450 ($\rho = -1.6$) and signifies that there is a substantial positive charge built up on the benzylic center during homolytic cleavage.[15] Regarding the nature of the bond cleavage event, the magnitude of the ρ value is in good agreement with a hydrogen-atom-transfer (HAT) model rather than an electron-transfer, proton-transfer reaction, where a larger substituent effect (more negative ρ value) would be expected. However, the observed KIE was smaller than what is typically expected for HAT reactions with similar ferryls.[5]

The first-order decay of the ferryl **5** at later time points is consistent with the decomposition reaction being unimolecular and not bimolecular with respect to **5**. In order to probe this process further, data were collected over a variable concentration range ([Fe] = 0.8−1.7 mM),[16] and these data were evaluated against several theoretical models using the program *DynaFit* (see the SI for further details).[17] The data fit best to a two-step process, where formation of the ferryl was treated as a bimolecular reaction and decay of the ferryl

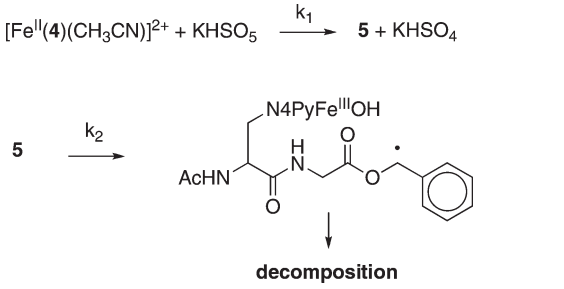

Figure 3. Proposed mechanism for the generation and decomposition of the ferryl−peptide conjugate **5**.

was considered a unimolecular reaction (Figure 3). Accordingly, second- and first-order rate constants of 5.2(4) M^{-1} s^{-1} and 5.9(1) × 10^{-4} s^{-1} were determined for k_1 and k_2, respectively. The first-order rate constant k_2 determined by this method was within reasonable error of the rate constant measured from the slope of the ln(Abs) vs time plot shown in Figure 1b (Table 1, entry 1), which confirms that the slope can be used to estimate k_2. The proposal that the decay of **5** is an intramolecular process is further supported by the fact that the addition of 1 equiv of benzyl acetate or benzyl alcohol to **5** has no effect on its rate of decomposition (Table S2 in the SI). However, rates do change slowly between 5 and 10 equiv of external substrate added, consistent with a unimolecular reaction becoming competitive with a bimolecular pathway only at higher concentrations of external substrate.

In conclusion, ferryls can be conjugated to peptides, and their stability can be controlled by changing the nature of a remote functional group. An intramolecular pathway is proposed for the decay of a ferryl−peptide conjugate. Studies are now underway in our laboratory to understand and define the functional group compatibility of ferryl groups in larger peptides, in terms of both their identity and their spatial relationship to the ferryl center. Furthermore, the methodology disclosed herein is expected to be useful for the synthesis of peptides or proteins that contain these metal-binding units.

Acknowledgment. We thank Alyssa Yousif for the preparation of synthetic intermediates, Dr. Domenico Gatti for assistance with the DynaFit software, and Wayne State University for its generous support of this research.

Supporting Information Available: Experimental procedures for the preparation of **1**−**10**, including characterization data and kinetic fits. This material is available free of charge via the Internet at http://pubs.acs.org.

(13) Guengerich, F. P. *J. Biol. Chem.* **1987**, *262*, 8459–8462.
(14) de Visser, S. P.; Oh, K.; Han, A.-R.; Nam, W. *Inorg. Chem.* **2007**, *46*, 4632–4641.
(15) Blake, R. C. II; Coon, M. J. *J. Biol. Chem.* **1981**, *256*, 12127–12133.
(16) Data were not collected at lower concentrations because of the low extinction coefficient of **5**.
(17) Kuzmic, P. *Anal. Biochem.* **1996**, *237*, 260–273.